journal

J. Am. Ceram. Soc., **81** [5] 1215–20 (1998)

$Ag–Bi_{1.5}Y_{0.5}O_3$ Composite Cathode Materials for $BaCe_{0.8}Gd_{0.2}O_3$-Based Solid Oxide Fuel Cells

Zhonglin Wu* and Meilin Liu*

School of Materials Science and Engineering, Georgia Institute of Technology, Atlanta, Georgia 30332-0245

$Ag–Bi_{1.5}Y_{0.5}O_3$ composites exhibit high electronic and ionic conductivities when the volume fraction of the silver phase is properly chosen, indicating that these composites are candidate cathode materials for solid-state ionic devices. In this study, the chemical and thermal compatibilities between $Ag–Bi_{1.5}Y_{0.5}O_3$ composites and $BaCe_{0.8}Gd_{0.2}O_3$ electrolyte are studied at intermediate temperatures. Furthermore, the electrochemical properties of the interfaces between the composites and the electrolyte are characterized under various conditions using impedance spectroscopy. The stability of the electrodes is estimated from the time dependence of the interfacial resistances. Results indicate that $Ag–Bi_{1.5}Y_{0.5}O_3$ composites are promising cathode materials for solid oxide fuel cells based on $BaCe_{0.8}Gd_{0.2}O_3$ electrolyte at intermediate temperatures.

I. Introduction

SOLID OXIDE FUEL CELLS (SOFCs) based on yttria-stabilized zirconia (YSZ) are operated typically at temperatures close to 1000°C.[1,2] Problems associated with such high temperatures include thermal stresses at electrolyte–electrode interfaces, interdiffusion between cell components, and degradation in cell performance. The replacement of YSZ with an ionic conductor having adequate conductivity at intermediate temperatures (550°–800°C) can improve cell stability over prolonged operation.[3,4] Gadolinium-doped barium cerates have been identified as one of the most promising electrolyte materials for intermediate-temperature SOFCs because of their high ionic conductivity at intermediate temperatures and good stability in the fuel cell environment.[5] The use of a new electrolyte, however, requires new electrodes that are compatible with that electrolyte. In many cases, the performance of an SOFC is not limited by the electrolyte but by the electrodes or the electrode–electrolyte interfaces. The catalytic activity or interfacial resistance of an electrode is an important factor that controls the performance of an SOFC. This is particularly true for an SOFC to be operated at intermediate or low temperatures, because electrode materials are typically less active catalytically at lower temperatures.[6–8] Furthermore, binding, thermal compatibility, and potential interdiffusion between electrode and electrolyte are critical factors that determine the stability of the developed electrodes for a particular electrolyte.

Metals with high catalytic activity and good stability at high temperatures—such as platinum, gold, and palladium—have been studied as electrode materials for YSZ-based SOFCs. However, these metals are too expensive and impractical for commercial SOFCs. Silver, on the other hand, is much less expensive and has excellent catalytic activity for oxygen reduction. Unfortunately, silver is not appropriate for high-temperature SOFCs because of its high evaporation rate at high temperatures.[9,10] Accordingly, cathode materials developed for YSZ-based SOFCs are primarily limited to perovskite oxides based on $LaMnO_3$ and $LaCoO_3$.

SOFCs based on barium cerates are to be operated at intermediate temperatures. The evaporation rate of silver is ~0.3 μm/year at 750°C,[4] and it decreases dramatically with reduction in temperature. This makes silver an acceptable electrode materials for intermediate-temperature SOFCs. However, two major problems remain when pure silver is used as an electrode for barium cerate-based SOFCs. First, pure silver has poor adhesion to the barium cerate electrolyte because of a large mismatch in thermal expansion coefficients between the two materials. Second, silver electrode readily densifies at relatively low temperatures (850°–900°C, at which electrodes are processed), resulting in a dense electrode with little porosity. This significantly reduces the number of gas–metal–electrolyte triple-phase points or boundaries and severely limits the electrode performance.

The use of a silver–ceramic composite electrode, however, can overcome these problems. Metal–ceramic composite materials can be highly conductive when the volume fraction of the metal is properly chosen.[11] Addition of a ceramic phase to silver can prevent the electrode from densifying, and the electrode can retain a porous structure during processing and operation.[12] The retained porous microstructure is essential to the performance of the electrode, because the electrochemical reaction must take place at the triple-phase points or boundaries among silver, $Bi_{1.5}Y_{0.5}O_3$, and gas or among silver, $BaCe_{0.8}Gd_{0.2}O_3$, and gas. The existence of pores greatly increases the number of these points or boundaries. Oxygen-gas transport through the electrode or near the triple-phase boundaries also is facilitated by the existence of pores. A properly chosen ceramic phase also can improve the thermal compatibility and adhesion between the electrode and the electrolyte. Furthermore, if the selected ceramic phase is an ionic (or mixed) conductor, the metal–ceramic composite may exhibit both ionic and electronic conduction, extending the electrochemical reaction sites beyond the electroyte–electrode interfaces, possibly to the entire electrode–gas interfaces. Thus, the preferred ceramic phases are an ionic conductor or a mixed ionic–electronic conductor. It has been reported that yttria-stabilized bismuth oxide (YSB) with composition $Bi_{1.5}Y_{0.5}O_3$[13] has high ionic conductivity, and bismuth oxide-based mixed conductors (e.g., Ag-YSB) exhibit very high oxygen permeability, particularly at intermediate temperatures.[14] Dense membranes of $Bi_{1.5}Y_{0.5}O_3$ and silver composite have been developed successfully and optimized for oxygen separation,[13] demonstrating the compatibility between silver and $Bi_{1.5}Y_{0.5}O_3$.

The feasibility of using porous $Ag–Bi_{1.5}Y_{0.5}O_3$ composites as cathodes for barium cerate-based SOFCs is investigated in this study. The performance of prepared composite electrodes is evaluated using cells of $Ag–Bi_{1.5}Y_{0.5}O_3|BaCe_{0.8}Gd_{0.2}O_3|Ag–Bi_{1.5}Y_{0.5}O_3$ under various conditions.

W. Huebner—contributing editor

Manuscript No. 191144. Received March 25, 1997; approved August 25, 1997.
Supported by the National Science Foundation under Award No. DMR-9357520 and Electric Powder Research Institute under Contract No. RP 1676-19.
*Member, American Ceramic Society.

II. Experimental Procedure

Bismuth oxide powder (99.9%, Aldrich Chemical Co., Milwaukee, WI) and Y_2O_3 powder (99.9%, Aldrich Chemical Co.) were ball milled in alcohol for up to 24 h. The slurry was dried in air at 70°C, and the resulting powder was passed through a 120 mesh sieve before calcination at 750°C in air for 10 h to form YSB with a composition of $Bi_{1.5}Y_{0.5}O_3$. The calcined $Bi_{1.5}Y_{0.5}O_3$, with cubic fluorite structure, as confirmed by X-ray diffractometry, then was mixed with an appropriate amount of Ag_2O powder (99%, Alfa Aesar Johnson Matthey, Ward Hill, MA), 35 wt% turpentine, and 5–7 wt% peanut oil to form a slurry. The mixture was ball milled until a good-quality paste was obtained. The Ag_2O–$Bi_{1.5}Y_{0.5}O_3$ pastes then were screen printed on both sides of $BaCe_{0.8}Gd_{0.2}O_3$ electrolyte pellets and subsequently fired at 850°–900°C for 5–30 min. Ag_2O decomposed to silver during firing. The use of Ag_2O, rather than metallic silver, improved the catalytic activity of the electrode and increased the porosity of the electrode because of the decomposition of Ag_2O during the firing of the electrode. The volume fractions of silver in the composites were varied from 25 to 85 vol%. Pure-silver electrodes were prepared for direct comparison using similar procedures and tested under similar conditions used for the composite electrodes.

The microstructures of the composite electrodes were studied using field-emission scanning electron microscopy (SEM) (Model S-800, Hitachi, Ltd., Tokyo, Japan) equipped with energy-dispersive spectroscopy (Quantum, Kevex Corp., Foster City, CA). A statistical point-counting method in quantitative stereology[15] was used to estimate the porosity in the composite electrodes. The diffusion of elements across the electrode–electrolyte interface was revealed using the X-ray dot-mapping technique. The electrochemical behavior of Ag–$Bi_{1.5}Y_{0.5}O_3$|$BaCe_{0.8}Gd_{0.2}O_3$|Ag–$Bi_{1.5}Y_{0.5}O_3$ cells was investigated using a computerized impedance analysis system, consisting of a frequency analyzer (Model 1255, Solartron, Allentown, PA) and an electrochemical interface (Model 1286, Solartron) at temperatures ranging from 550° to 750°C and in the millihertz to megahertz frequency range. The impedances of the cells were determined under different partial pressures of oxygen and at different polarization voltages. Gas mixtures having different oxygen partial pressures used in the measurement were obtained by mixing oxygen with argon through a gas meter. Cathodic overpotentials of the symmetrical cells in dry air, wet air, and oxygen were determined using four-probe impedance and polarization techniques.

III. Results and Discussion

(1) Microstructure, Interdiffusion, and Adhesion

Figures 1(A) and (B) are SEM photographs showing surface and cross-sectional views of an electrode with a composition of 55 vol% Ag and 45 vol% $Bi_{1.5}Y_{0.5}O_3$ deposited on a $BaCe_{0.8}Gd_{0.2}O_3$ pellet. The thickness of the electrode is ~10 μm. The distribution of silver and $Bi_{1.5}Y_{0.5}O_3$ seems to be uniform. The electrode is relatively porous, and quantitative analysis of the microstructure indicates that the porosity is ~21%. In contrast, the microstructure of a pure-silver electrode, which was prepared in parallel to the composite electrode under similar conditions, is quite different from that of the composite electrode. The silver electrode appears to be pore free and consists of densely packed large grains. This type of microstructure is highly undesirable. Therefore, addition of YSB grains acts as a silver grain growth inhibitor and, thus, maintains the porosity.

In general, diffusion of elements across the interface between the electrode and the electrolyte during processing (at 850°–900°C) and operation (at 750°C or lower) could alter the interface properties, binding strength, and, possibly, the conducting behavior of both electrode and electrolyte. $Bi_{1.5}Y_{0.5}O_3$ and $BaCe_{0.8}Gd_{0.2}O_3$ pellets were prepared to study the diffusion phenomena. Each pellet was ground and polished to 0.05 μm. The two types of pellets were put together with the polished surfaces facing each other to form a diffusion couple. The diffusion couples then were annealed at 900° and 750°C for 1 and 4 h. The elemental distribution on cross sections of annealed samples was revealed using X-ray mapping. Figure 2 shows the elemental distribution on a cross section of a diffusion couple annealed at 900°C for 1 h (Fig. 2(A)) and 4 h (Fig. 2(B)). It appears that only bismuth diffused significantly into the barium cerate electrolyte. As the annealing time increased, bismuth diffused deeper into the barium cerate. At 750°C, however, no interdiffusion of elements between the Ag–$Bi_{1.5}Y_{0.5}O_3$ composite and the $BaCe_{0.8}Gd_{0.2}O_3$ electrolyte was observed. The diffusion of bismuth into $BaCe_{0.8}Gd_{0.2}O_3$ at the processing temperature, together with the low melting point of $Bi_{1.5}Y_{0.5}O_3$, increased the binding strength between the electrode and the electrolyte. Because the resistance of bismuth-doped barium cerate in air was only slightly higher than that of barium cerate itself,[16] the effect of this diffusion on the electrical properties was small.

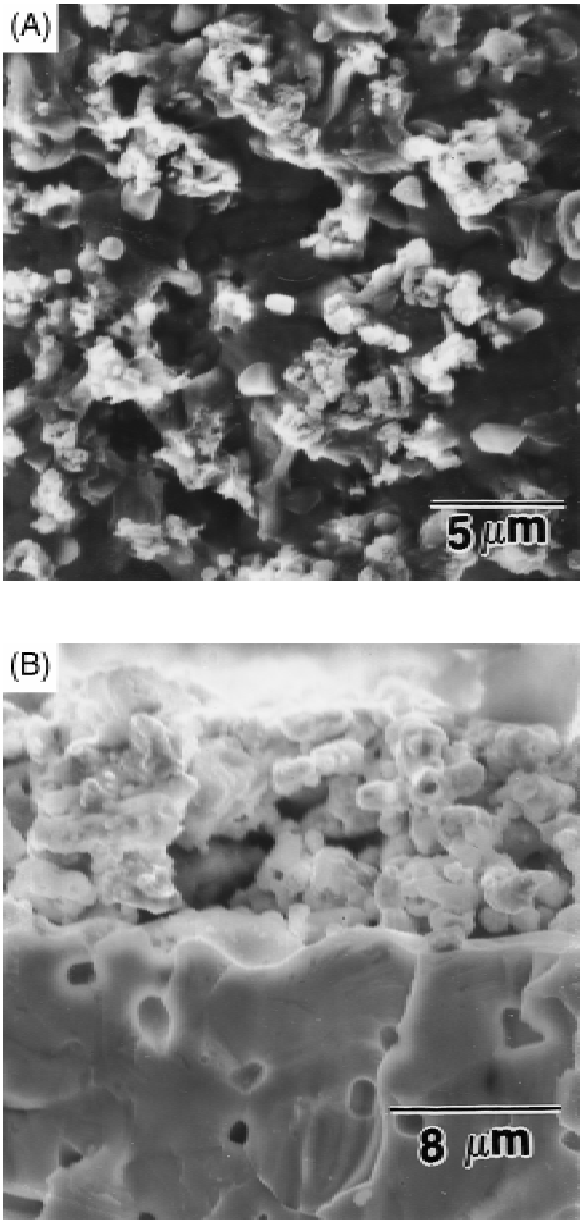

Fig. 1. (A) Surface view and (B) cross-sectional view of a composite electrode with composition of 55 vol% Ag–45 vol% $Bi_{1.5}Y_{0.5}O_3$ deposited on a $BaCe_{0.8}Gd_{0.2}O_3$ pellet.

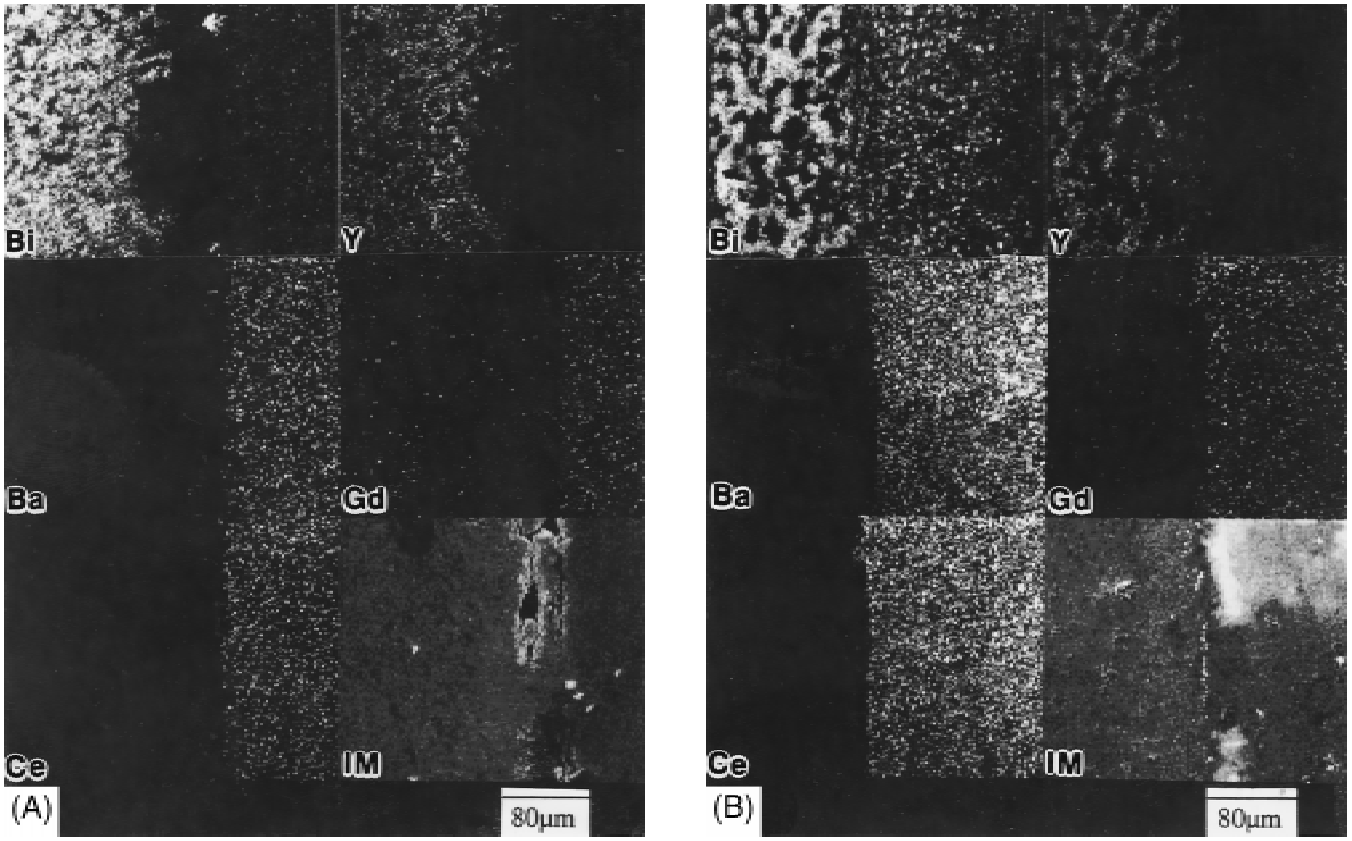

Fig. 2. Elemental distribution on a cross section of $Bi_{1.5}Y_{0.5}O_3$–$BaCe_{0.8}Gd_{0.2}O_3$ diffusion couples annealed at 900°C for (A) 1 h and (B) 4 h.

As reported earlier,[12] the adhesion of the silver electrode to the $BaCe_{0.8}Gd_{0.2}O_3$ electrolyte was quite poor because of the large thermal expansion mismatch between the two materials: the thermal expansion coefficient of $BaCe_{0.8}Gd_{0.2}O_3$ is ~9 × 10^{-6}/°C and the thermal expansion coefficient of silver is ~19 × 10^{-6}/°C. The bonding between a pure silver electrode and the electrolyte could not withstand repeated heating–cooling cycles from room temperature to 750°C; the silver layer usually delaminated after the second heating–cooling cycle. In contrast, the Ag–YSB composite electrode retained good adhesion to the $BaCe_{0.8}Gd_{0.2}O_3$ electrolyte after repeated heating–cooling cycles.

(2) Effect of Volume Fraction of Silver in the Composite Electrode

Different amounts of Ag_2O were mixed with $Bi_{1.5}Y_{0.5}O_3$ to vary the volume fraction of silver in the composite electrodes. All electrodes prepared were highly conductive except the one containing 25 vol% silver. This is consistent with the prediction of the effective medium percolation theory (EMPT),[11,17] which indicates that the volume fraction of the randomly distributed metal phase should exceed ⅓ to form a continuous metal phase.

Figure 3(A) shows a series of impedance spectra, measured at 750°C in air, of the cells having Ag–$Bi_{1.5}Y_{0.5}O_3$ composite electrodes with different volume fractions of silver. At least two depressed semicircles are observed in each spectrum. Because the same electrolyte was used in all cells studied, the observed changes in impedance spectra, as shown in Fig. 3(A), are caused primarily by the variation in volume fraction of silver in the electrodes. The intercept of the impedance locus with the real axis at high frequencies corresponds to the bulk resistance of the electrolyte (R_b), and the intercept of the loops with the real axis at low frequencies is the total resistance (R_T) of the cell. The two depressed semicircles correspond to the electrochemical processes occurring at the electrode–electrolyte interfaces. Because the ionic transference number (t_i) under the test conditions in this article is ~0.6,[18] the interfacial resistance (R_p) can be determined from[18]

$$R_p = \frac{R_T - R_b}{t_i\left[1 - \frac{R_T}{R_b}(1 - t_i)\right]} \tag{1}$$

Figure 3(B) shows the resistances of the electrode–electrolyte interfaces calculated from the impedance spectra, using Eq. (1). As expected, the interfacial resistance of the composite is a strong function of the volume fraction of silver. The optimal volume fraction of silver seems to be 55%–60%. The electrode with a composition of 55 vol% Ag–45 vol% $Bi_{1.5}Y_{0.5}O_3$ shows the lowest interfacial resistance or the highest exchange current density among the compositions studied. Accordingly, a composite of this composition was selected for further investigation.

This result also is within the expectation of the EMPT, which predicts that both ionic and electronic conductivities are reasonably high when the volume fraction of the metal phase is within ⅓ to ⅔ for a dense metal–ceramic composite. However, the EMPT theory predicts that the highest mixed conductivity should be reached when the volume fraction of the randomly distributed metal phase is slightly higher than ⅓ for a dense composite. The optimum volume fraction of metal in the composite electrode seems not to be at that point. The main reason for the discrepancy is that the existence of pores decreases the actual volume percent of silver in the electrode layer. For example, the actual volume fraction of silver would be decreased from 55% in a dense composite to 44% if the porosity of the composite is 20%. Another possible reason is that silver has a high catalytic property and a large amount of silver phase can improve the inherent catalytic activity of the electrode. The overall performance of a porous electrode not only is determined by the mixed ionic–electronic transport properties in the solid phase of the electrode but also by the inherent catalytic

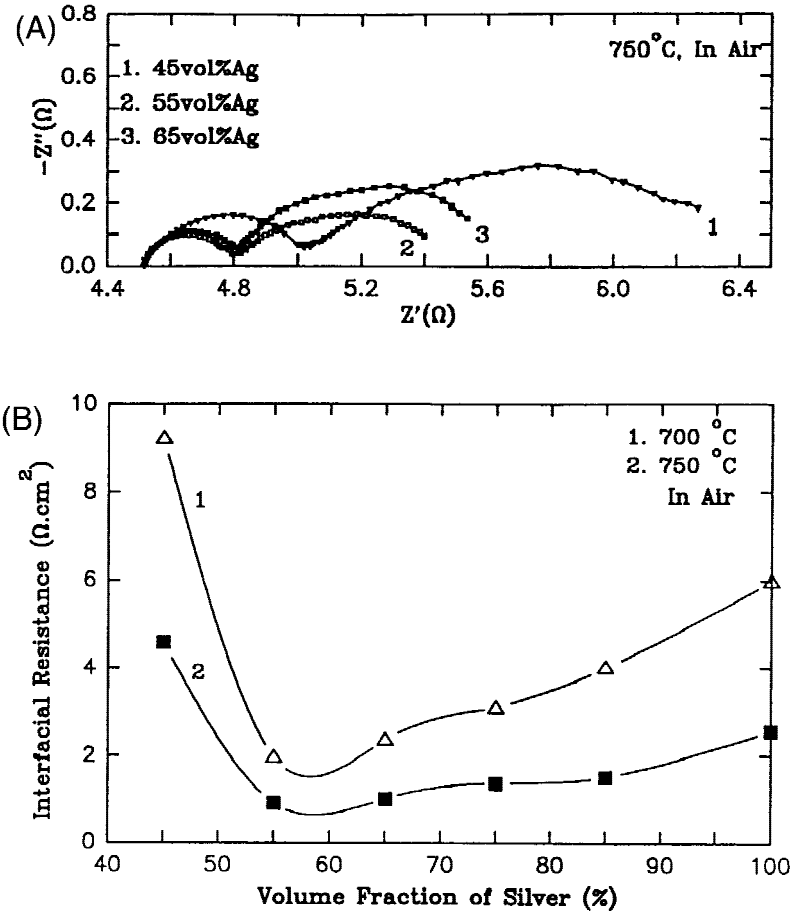

Fig. 3. Dependence of (A) impedance spectra and (B) interfacial resistances on the volume fraction of silver in Ag–$Bi_{1.5}Y_{0.5}O_3$ composite electrodes as measured in a cell with a configuration of Ag–$Bi_{1.5}Y_{0.5}O_3$|$BaCe_{0.8}Gd_{0.2}O_3$|Ag–$Bi_{1.5}Y_{0.5}O_3$ (electrode area of 0.637 cm^2 and electrolyte thickness of 0.162 cm).

property of the triple-phase points or boundaries and by the gas transport to or away from the triple-phase points or boundaries.

(3) Stability, Activation Energy, and Effect of Polarization

Two major concerns for using Ag–YSB electrodes are reduction in porosity and specific surface area due to the densification of silver and diffusion of bismuth into $BaCe_{0.8}Gd_{0.2}O_3$ electrolyte at operating temperatures. If considerable electrode densification or bismuth diffusion takes place during operation, degradation in the electrode performance can occur. A cell with 55 vol% Ag–45 vol% $Bi_{1.5}Y_{0.5}O_3$ electrodes was tested at 750°C in air for 100 h. The interfacial resistances increased ~2.5% in the initial stage and then remained relatively constant. This implies that the effect of electrode densification and bismuth diffusion on interfacial properties at operating temperatures is small. The changes in the bulk resistance of the $BaCe_{0.8}Gd_{0.2}O_3$ electrolyte also are within experimental error, indicating that the diffusion of bismuth into $BaCe_{0.8}Gd_{0.2}O_3$ has no significant effect on the electrolyte performance.

Figure 4 shows impedance spectra of a cell, 55 vol% Ag–45 vol% $Bi_{1.5}Y_{0.5}O_3$|$BaCe_{0.8}Gd_{0.2}O_3$|55 vol% Ag–45 vol% $Bi_{1.5}Y_{0.5}O_3$, measured at temperatures from 500° to 800°C in air. Figure 5 shows an Arrhenius plot of the interfacial resistances determined from the impedance spectra. A single slope implies that the same reaction mechanism controls the overall electrode behavior in the temperature range studied. The activation energy for the interfacial reaction is determined to be 119 kJ/mol (or 1.23 eV), which is slightly less than that of a pure silver electrode (137 kJ/mol).

The impedance spectra of the cells with 55 vol% Ag–45 vol% $Bi_{1.5}Y_{0.5}O_3$ electrodes were measured at 750°C in air under the influence of different polarization voltages. Both semicircles in each impedance spectrum were changed when a bias was applied; the higher the applied bias, the smaller the sizes of the impedance loops. This indicates that both loops are related to the interfaces. Figure 6 shows the average overpotential across an electrode–electrolyte interface as a function of cell current. The overpotentials are the mean values obtained by averaging the potential drops across the cathode–electrolyte interface and the anode–electrolyte interface during polarization measurements. Because the applied voltage is relatively small, it is reasonable to assume that the overpotential drop across the cathode is similar to that across the anode. Compared to the pure silver electrode, the overpotential at the composite electrode is significantly reduced. For example, when a current of 40 mA/cm^2 is applied, the overpotential at the composite electrode is ~52% of that at the pure silver electrode.

(4) Effect of Oxygen Partial Pressure

The overall cathodic reaction in a fuel based on the $BaCe_{0.8}Gd_{0.2}O_3$ electrolyte and the composite electrode can be written as

$$O_2 + 2V_O^{\cdot\cdot} + 4e' \rightarrow 2O_O^X \quad (2)$$

Therefore, the interfacial resistance or the exchange current density depends critically on the oxygen partial pressure. In general, the dependence of exchange current density on the oxygen partial pressure (p_{O_2}) can be expressed as[19]

$$i_O = kp_{O_2}^{\gamma} \quad (3)$$

where k is a reaction constant independent of p_{O_2} and γ an exponent dependent on the reaction mechanism (reaction path and rate-limiting step). The impedance spectra of the cells with 55 vol% Ag–45 vol% $Bi_{1.5}Y_{0.5}O_3$ composite electrodes were measured at different oxygen partial pressures. Figure 7 shows the exchange current densities, determined from impedance spectra,[20] as a function of oxygen partial pressure at 660°,

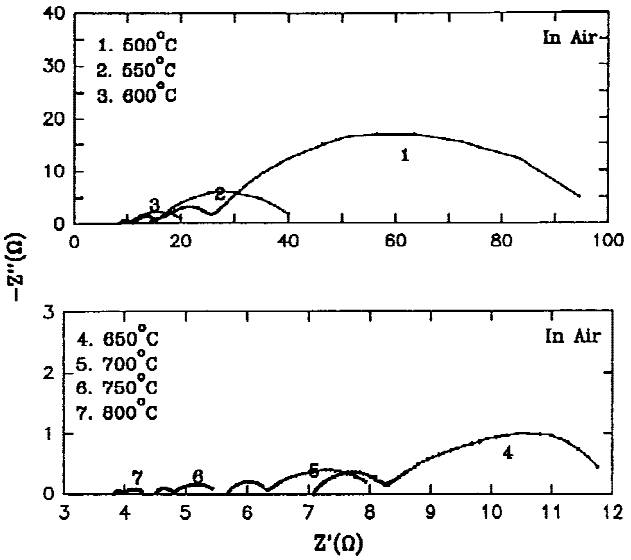

Fig. 4. Impedance spectra of a cell with a configuration of 55 vol% Ag–45 vol% $Bi_{1.5}Y_{0.5}O_3$|$BaCe_{0.8}Gd_{0.2}O_3$|55 vol% Ag–45 vol% $Bi_{1.5}Y_{0.5}O_3$ at different temperatures (electrode area of 0.637 cm^2 and electrolyte thickness of 0.162 cm).

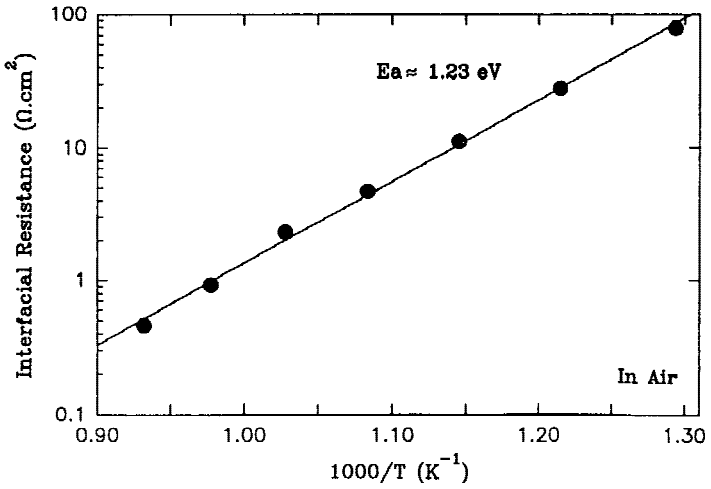

Fig. 5. Interfacial resistance as a function of temperature (electrode area of 0.637 cm^2 and electrolyte thickness of 0.162 cm).

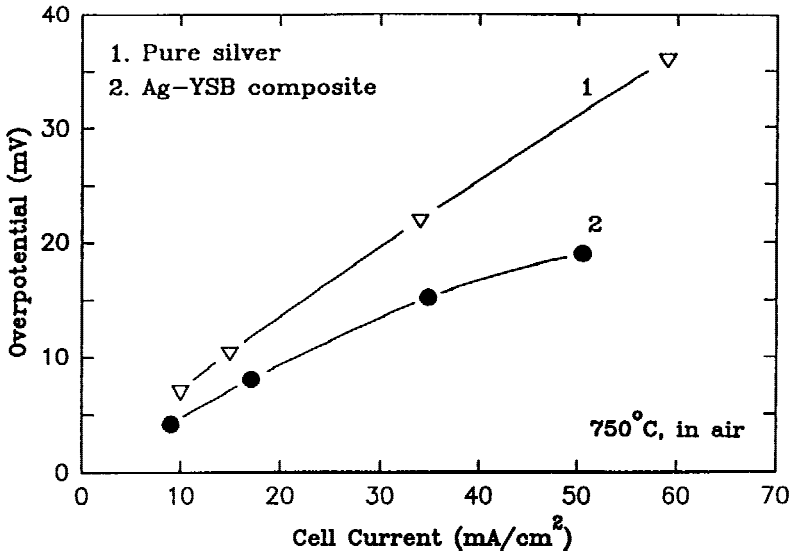

Fig. 6. Overpotential at electrode–electrolyte interface as a function of the cell current at 750°C in air.

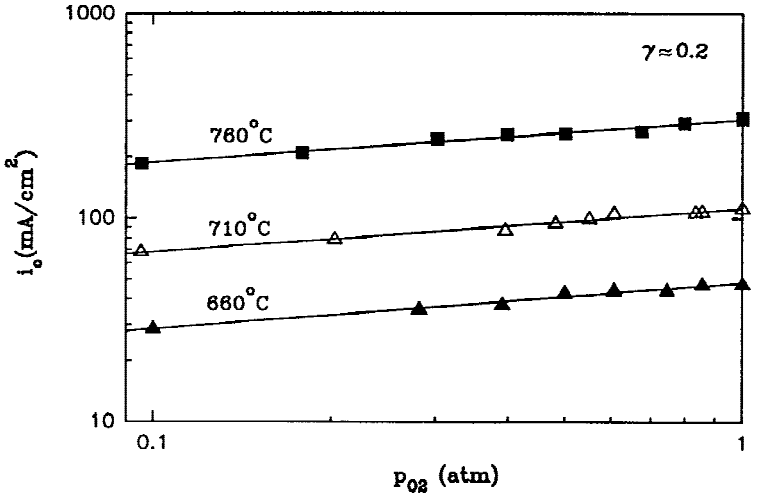

Fig. 7. Dependence of interfacial resistance on oxygen partial pressure (electrode area of 0.637 cm^2 and electrolyte thickness of 0.162 cm).

710°, and 760°C. The slopes of the regressive lines are almost identical for the three temperatures ($\gamma \approx 0.2$). This again demonstrates that the same reaction mechanism prevails in the temperature range studied. The slopes of these plots are important to the determination of the rate-limiting step in the electrode reaction. Possible reaction mechanisms can be deduced from the comparison of the theoretical formulations to the experimental results. The detailed electrode kinetics remains under investigation.

IV. Conclusions

The performance of Ag–$Bi_{1.5}Y_{0.5}O_3$ composite electrodes depends on the volume fraction of silver. The composites containing 55–60 vol% silver exhibit the lowest interfacial resistance or the highest catalytic activity for oxygen reduction and evolution. Porosity of the composite electrode also is important. Certain porosity is required in the composite electrode to allow sufficient gas transport through the electrode and to ensure adequate triple-phase points or boundaries to facilitate electrochemical reactions. Compared to a pure silver electrode, a composite electrode with a composition of 55 vol% Ag–45 vol% $Bi_{1.5}Y_{0.5}O_3$ exhibits higher exchange current density and lower overpotential as well as better binding strength with barium cerate electrolyte. Thus, composites of silver and $Bi_{1.5}Y_{0.5}O_3$ are promising cathode materials for $BaCe_{0.8}Gd_{0.2}O_3$-based SOFCs to be operated at intermediate temperatures.

References

[1]Advances in Ceramics, Vol. 24, *Science and Technology of Zirconia III*. Edited by S. Sōmiya, N. Yamamoto, and H. Yanagida. American Ceramic Society, Westerville, OH, 1988.

[2]T. H. Etsell and S. N. Flengas, ''The Electrical Properties of Solid Oxide Electrolytes,'' *Chem. Rev.*, **70**, 339–76 (1970).

[3]B. C. H. Steele, ''Mass Transport in Materials Incorporated in Electrochemical Energy Conversion Systems,'' *Solid State Ionics*, **12**, 391–406 (1984).

[4]S. A. Barnett, ''New Solid Oxide Fuel Cell Designed Based on Thin Film Electrolytes,'' *Energy*, **15**, 1–9 (1990).

[5]N. Taniguchi, K. Hatoh, J. Niikura, T. Gamo, and H. Iwahara, ''Proton Conductive Properties of Gadolinium-Doped Barium Cerates at High Temperatures,'' *Solid State Ionics*, **53–56**, 998–1003 (1992).

[6]M. Liu and A. Khandkar, ''Considerations in Design and Characterization of Solid-State Electrochemical Systems,'' *Solid State Ionics*, **52**, 3–13 (1992).

[7]M. Watanabe, H. Uchida, M. Shibata, N. Mochizuki, and K. Amikura, ''High-Performance Catalyzed-Reaction Layer for Medium Temperature Operating Solid Oxide Fuel Cells,'' *J. Electrochem. Soc.*, **141**, 342–46 (1994).

[8]M. Suzuki, H. Sasaki, S. Otashi, A. Kajimura, N. Sugiura, and M. Ippommatsu, ''High-Performance Solid Oxide Fuel Cell Cathode Fabricated by Electrochemical Vapor Deposition,'' *J. Electrochem. Soc.*, **141**, 1928–31 (1994).

[9]J. Van Herle and A. J. McEvoy, ''Oxygen Diffusion through Silver Cathodes for Solid Oxide Fuel Cells,'' *J. Phys. Chem. Solids*, **55**, 339–47 (1994).

[10]E. Schouler, M. Kleitz, and C. Deportes, ''Capacitive Effects at an Oxygen–Silver-Stabilized Zirconia Interface,'' *J. Chim. Phys.*, **83**, 35–41 (1973).

[11]Z. Wu and M. Liu, ''Modeling of Ambipolar Transport Properties of Composite Mixed Ionic–Electronic Conductors,'' *Solid State Ionics*, **93**, 65–84 (1997).

[12]H. Hu and M. Liu, ''Silver–$BaCe_{0.8}Gd_{0.2}O_3$ Composites as Cathode Materials for SOFCs Using $BaCeO_3$-Based Electrolytes,'' *J. Electrochem. Soc.*, **143**, 859–64 (1996).

[13]A. M. Azad, L. Larose, and S. A. Akbar, ''Bismuth Oxide-Based Solid Electrolytes for Fuel Cells,'' *J. Mater. Sci.*, **29**, 4135–51 (1994).

[14]M. Liu, A. Joshi, Y. Shen, and K. Krist, ''Composite Mixed Ionic–Electronic Conductors for Oxygen Separation and Electrocatalysis,'' U.S. Pat. No. 5 478 444, 1995.

[15]E. E. Underwood, *Quantitative Microscopy*; p. 94. McGraw-Hill, New York, 1966.

[16]W. Rauch and M. Liu, ''Effect of Microstructure and Dopant on the Electrochemical Properties of Barium Cerate-Based Electrolytes''; pp. 146–65 in *Ceramic Membranes I*, PV 95–24. Edited by H. U. Anderson, A. C. Khandkar, and M. Liu. The Electrochemical Society, Pennington, NJ, 1996.

[17]D. G. Ast, ''Evidence for Percolation-Controlled Conductivity in Amorphous As_xTe_{1-x} Films,'' *Phys. Rev. Lett.*, **33**, 1042–45 (1974).

[18]M. Liu and H. Hu, ''Effect of Interfacial Resistance on Determination of Transport Properties of Mixed-Conducting Electrolytes,'' *J. Electrochem. Soc.*, **143**, L109–L112 (1996).

[19]M. Liu, ''Electrode Kinetics and Transport Properties of Mixed Ionic and Electronic Conductors''; pp. 191–215 in *Proceedings of First International Symposium on Ionic and Mixed Conducting Ceramics* (PV 91–12). Edited by T. A. Ramanaryanan and H. L. Tuller. The Electrochemical Society, Pennington, NJ, 1991.

[20]M. Liu, H. Hu, and W. L. Rauch, ''Ionic and Electronic Transport in $BaCe_{0.8}Gd_{0.2}O_3$ Solid Electrolytes''; see Ref. 16, pp. 199–220. □